Journal of Sound and Vibration (1998) **217**(2), 197–221
Article No. sv981741

FREE VIBRATION OF A CIRCULAR CYLINDRICAL SHELL FILLED WITH BOUNDED COMPRESSIBLE FLUID

KYEONG-HOON JEONG

Korea Atomic Energy Research Institute, *Taejon*, 305-600 *Korea*

AND

KWI-JA KIM

Woosong Technical College, *Taejon*, 300-100 *Korea*

(*Received* 10 *November* 1997, *and in final form* 16 *April* 1998)

This paper presents an analytical method for evaluating the linear free vibration of a circular cylindrical shell filled with bounded compressible fluid. The analytical method was developed by means of the finite Fourier series expansion method. The motion of compressible fluid coupled with the shell was determined by means of the linearized velocity potential flow theory. To clarify the validity of the analytical method, the coupled natural frequencies of a water-filled circular cylindrical shell with a clamped–clamped boundary condition were obtained by the analytical method and finite element analysis. Excellent agreement on the natural frequencies of the liquid-coupled shell structure was found. The results show that the natural frequencies decrease with an increase in fluid compressibility. However, the compressibility effect on the lower circumferential mode frequencies was found to be relatively significant. Additionally, it was found that the rigid bounding of fluid at the ends of the shell decreases the natural frequencies for the lower circumferential modes when compared with the sloshing fluid case.

© 1998 Academic Press

1. INTRODUCTION

This paper contains the modal analysis of a thin, circular cylindrical shell filled with compressible fluid, bounded by top and bottom rigid plates. The work arises as part of a project investigating the vibration of compressed gas storage tanks and pressurized water reactors filled with coolant. The fluid coupled shell systems have no free surface of fluid within the cylindrical tank. Many researchers have studied similar problems, both theoretically and experimentally. They treated the liquid contained within the shell as a sloshing fluid with a free surface instead of a bounded fluid. Stillman [1] approached the problem using the classical Rayleigh–Ritz method for a cantilevered cylindrical shell partially filled with an inviscid and incompressible liquid. Yamaki *et al*. [2] and Gonçalves and Ramos [3] developed an analytical method for the free vibration of a clamped cylindrical

0022–460X/98/420197 + 25 $30.00/0 © 1998 Academic Press

shell partially filled with an ideal fluid using the Galerkin procedure. Numerical solutions were produced by Lakis and Sinno [4] and Mikami and Yoshimura [5]. Han and Liu [6] considered tanks with axial non-uniformity in the thickness when studying the same problem. Jeong and Lee [7] studied the problem using a series expansion method. In addition, Gupta and Hutchinson [8], Zhu [9] and Huang [10] investigated the fluid-coupled shells using a continuum-based procedure and variational principle. Chen and Rosenberg [11] carried out a study of two concentrically located circular cylindrical shells containing incompressible fluids. However, the boundary conditions at the end of the fluid columns were not defined. Therefore, the fluid coupled with shells could flow out in an axial direction. All the above works assumed an incompressible, ideal fluid. An experimental study was carried out and verified with FEM by Mazuch *et al*. [12]. Application of the sloshing fluid boundary condition to the dynamic analysis of a cylindrical shell filled with bounded compressible fluid can produce some errors.

This paper extended the analytical approach developed by Jeong and Lee [7] by taking the compressibility and bounded boundary condition of the fluid into account. Therefore, it was not necessary to consider the fluid sloshing effect in the analysis. An example of applying the theoretical method to predict the coupled natural frequencies of a cylindrical shell filled with an inviscid compressible bounded fluid was provided and a finite element analysis was also conducted in order to verify the theoretical method. The effects of compressibility and the bounding of a fluid on the coupled natural frequencies were investigated.

2. THEORETICAL BACKGROUND

2.1. EQUATION OF MOTION AND BOUNDARY CONDITIONS OF THE SHELL

Consider a circular cylindrical shell containing compressible fluid covered by rigid end plates, as illustrated in Figure 1. The circular cylindrical shell has a mean radius R, height H, and wall thickness h. The Sanders' shell equations coupled with a fluid effect can be written as:

$$R^2u_{,zz} + \frac{(1-\mu)}{2}\left(1+\frac{k}{4}\right)u_{,\theta\theta} + R\left\{\frac{(1+\mu)}{2} - \frac{3(1-\mu)}{8}k\right\}v_{,z\theta} + \mu R w_{,z}$$

$$+ \frac{(1-\mu)}{2}Rk w_{,z\theta\theta} = \gamma^2 u_{,tt}, \tag{1a}$$

$$R\left\{\frac{(1+\mu)}{2} - \frac{3(1-\mu)}{8}k\right\}u_{,z\theta} + (1+k)v_{,\theta\theta} + \frac{(1-\mu)}{2}R^2\left(1+\frac{9k}{4}\right)v_{,zz}$$

$$-\frac{(3-\mu)}{2}R^2k w_{,zz\theta} + w_{,\theta} - k w_{,\theta\theta\theta} = \gamma^2 v_{,tt}, \tag{1b}$$

$$\frac{(1-\mu)}{2} Rku_{,z\theta\theta} + \mu Ru_{,z} - \frac{(3-\mu)}{2} R^2 kv_{,zz\theta} + v_{,\theta} + w + k(R^4 w_{,zzzz} + 2R^2 w_{,zz\theta\theta}$$

$$+ w_{,\theta\theta\theta\theta} - v_{,\theta\theta\theta}) = -\gamma^2 w_{,tt} + \frac{R^2 p}{D}, \tag{1c}$$

where the comma (,) denotes a partial derivative. The symbols used in the equations are listed in Appendix D.

When the shell is clamped at both ends, the boundary conditions are:

$$u = v = w = w_{,z} = 0 \qquad \text{at } z = 0 \quad \text{and} \quad z = H. \tag{2}$$

The other classical boundary conditions applicable to the cylindrical shell can be defined as equations (27) and (29).

The relationship between the forces acting on a section of a circular cylindrical shell and the displacement is given as:

$$N_z = D\left[u_{,z} + \frac{\mu}{R} v_{,\theta} + \frac{\mu}{R} w \right], \tag{3a}$$

$$N_{z\theta} = \frac{D(1-\mu)}{2}\left[\frac{1}{R}(1 - \tfrac{3}{4}k)u_{,\theta} + (1 + \tfrac{9}{4}k)v_{,z} - 3kw_{,z\theta} \right], \tag{3b}$$

$$Q_z = K\left[-\frac{(1-\mu)}{2R^3} u_{,\theta\theta} + \frac{(3-\mu)}{2R^2} v_{,z\theta} - \frac{(2-\mu)}{R^2} w_{,z\theta\theta} - w_{,zzz} \right], \tag{3c}$$

$$M_z = K\left[\frac{\mu}{R^2}(v_{,\theta} - w_{,\theta\theta}) - w_{,zz} \right], \tag{3d}$$

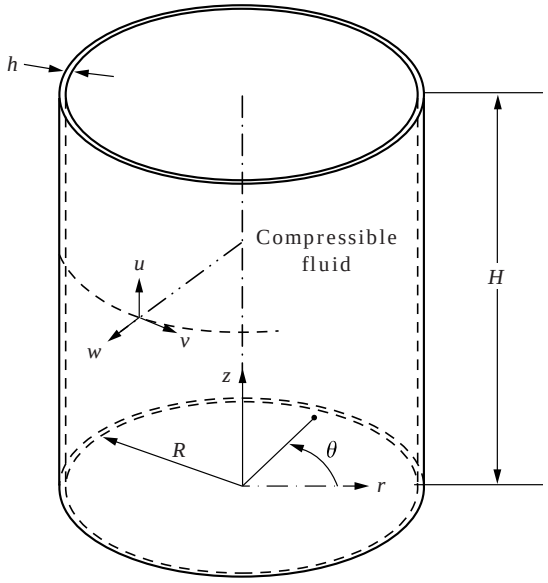

Figure 1. A circular cylindrical shell containing a bounded compressible fluid.

where $D = Eh/(1-\mu^2)$, $K = Eh^3/12(1-\mu^2)$ and N_z, $N_{z\theta}$, Q_z, M_z denote the membrane tensile force, effective membrane shear force, effective transverse shear force and bending moment per unit length, respectively.

2.2. MODAL FUNCTIONS

A general relation for the dynamic displacements in any mode of free vibration can be written in the following form for any circumferential mode number n:

$$u(z,\theta,t) = u(z)\cos n\theta \exp(\mathrm{i}\omega t), \qquad v(z,\theta,t) = v(z)\sin n\theta \exp(\mathrm{i}\omega t),$$

$$w(z,\theta,t) = w(z)\cos n\theta \exp(\mathrm{i}\omega t). \tag{4a–c}$$

Here $u(z)$, $v(z)$, and $w(z)$ are modal functions of the shell corresponding to the axial, tangential, and radial displacements, respectively. These modal functions along the axial direction can be written as a set of Fourier series [7, 13] that preserves the orthogonal properties.

$$u(z) = \sum_{m=1}^{\infty} A_{mn} \sin\left(\frac{m\pi z}{H}\right), \qquad v(z) = B_{on} + \sum_{m=1}^{\infty} B_{mn} \cos\left(\frac{m\pi z}{H}\right),$$

$$w(z) = C_{on} + \sum_{m=1}^{\infty} C_{mn} \cos\left(\frac{m\pi z}{H}\right). \tag{5a–c}$$

Here A_{mn}, B_{on}, B_{mn}, C_{on} and C_{mn} denote the unspecified Fourier coefficients which define the mode shapes of the shell. The modal function set of the Fourier series does not satisfy any particular boundary conditions at this time. However, the simple form of the series designated as the "SCC" set by Chung [13] can be appropriate for dealing with a general solution. The derivatives of modal functions can be obtained by the finite Fourier transform [14] or Stokes' transform [13]. The successive derivatives of the modal function series obtained by the transforms are listed in Appendix A. The derivatives for the sine and cosine series are used in the direct solution procedure of the shell equations. Additionally, the modal functions and their derivatives are coincident with the motion of the contained fluid.

2.3. EQUATION OF COMPRESSIBLE FLUID MOTION

The contained fluid does not maintain a free surface since it is bounded by the rigid end plates at both ends of the shell. The inviscid, irrotational and compressible fluid motion due to the shell vibration is described by the general velocity potential Φ:

$$\Phi_{,rr} + \frac{1}{r}\Phi_{,r} + \frac{1}{r^2}\Phi_{,\theta\theta} + \Phi_{,zz} = \frac{1}{c^2}\Phi_{,tt}, \tag{6}$$

where c is the speed of sound in the fluid medium, which is equal to $\sqrt{B/\rho_o}$. B is the bulk modulus of the elasticity of fluid, and ρ_o stands for the density of fluid. It is possible to separate the function Φ with respect to z by observing that the rigid plates attached to both ends of the shell prevent the fluid from moving to the z direction. Thus:

$$\Phi(z, r, \theta, t) = \mathrm{i}\omega\phi(r, \theta, z)\exp(\mathrm{i}\omega t) = \mathrm{i}\omega\phi(r, \theta)f(z)\exp(\mathrm{i}\omega t), \qquad \mathrm{i} = \sqrt{-1}, \quad (7)$$

where ω is the coupled natural frequency of the shell. Substitution of equation (7) into the partial differential equation (6) gives

$$\frac{\left[\phi(r, \theta)_{,rr} + \dfrac{1}{r}\phi(r, \theta)_{,r} + \dfrac{1}{r^2}\phi(r, \theta)_{,\theta\theta} + \left(\dfrac{\omega}{c}\right)^2\phi(r, \theta)\right]}{\phi(r, \theta)} = -\frac{f(z)_{,zz}}{f(z)} = \left(\frac{m\pi}{H}\right)^2. \quad (8)$$

When one considers the requirement that the velocity potential at $r = 0$ should be finite, it is possible to solve the partial differential equation (8) by the separation of variables technique:

$$\phi(r, z, \theta) = \left[D_{on}\, J_n\left(\frac{\omega}{c}\, r\right) + \sum_{m=1}^{\infty} D_{mn}\, I_n(\alpha_{mn} r)\cos\left(\frac{m\pi z}{H}\right)\right]\sin n\theta,$$

$$\text{for} \quad \frac{m\pi}{H} \geqslant \frac{\omega}{c} \quad (9a)$$

and

$$\phi(r, z, \theta) = \left[D_{on}\, J_n\left(\frac{\omega}{c}\, r\right) + \sum_{m=1}^{\infty} D_{mn}\, J_n(\alpha_{mn} r)\cos\left(\frac{m\pi z}{H}\right)\right]\sin n\theta,$$

$$\text{for} \quad \frac{m\pi}{H} < \frac{\omega}{c}, \quad (9b)$$

where $J_n(\,)$ is the Bessel function of the first kind of order n, and $I_n(\,)$ is the modified Bessel function of the first kind of order n. ϕ represents the spatial velocity potential for the contained fluid. α_{mn} is related to the speed of sound in the fluid:

$$\alpha_{mn} = \sqrt{\left|\left(\frac{m\pi}{H}\right)^2 - \left(\frac{\omega}{c}\right)^2\right|}. \quad (10)$$

The boundary condition of impermeable rigid surfaces on the top and bottom of the shell will give zero fluid velocity in the axial direction, so:

$$\phi_{,z}|_{z=0} = \phi_{,z}|_{z=H} = 0, \qquad 0 \leqslant r \leqslant R. \quad (11)$$

In addition, when the thickness of the shell is negligible compared to the diameter of the shell, the boundary condition assures the contact between the wall surface of the shell and the fluid. The requirement is given as:

$$\phi_{,r}|_{r=R} = -w(z, \theta), \qquad 0 \leqslant z \leqslant H. \tag{12}$$

From equation (12), the unspecified Fourier coefficients D_{on} and D_{mn} in equation (9), associated with the fluid motion, can be described in terms of the Fourier coefficients C_{on} and C_{mn} associated with the radial displacement of the shell. Further, the hydrodynamic pressure exerted by the fluid on the wetted shell surface can be given as:

$$p(z, \theta, t) = \rho_o \omega^2 \phi(R, z, \theta) \exp(\mathrm{i}\omega t). \tag{13}$$

Now, the normalized force due to the hydrodynamic pressure on the wetted shell surface, namely, $R^2 p(z, \theta, t)/D$ in equation (1c), can be reduced in terms of the Fourier coefficients, C_{on} and C_{mn} associated with the radial displacement of the cylindrical shell:

$$\frac{R^2 p(z, \theta, t)}{D} = \left[Y_1 \, C_{on} + \sum_{m=1}^{\infty} Z_m \, C_{mn} \cos\left(\frac{m\pi z}{H}\right) \right] \sin n\theta \, \exp(\mathrm{i}\omega t), \tag{14}$$

where

$$Y_1 = -\left(\frac{c}{\omega}\right)\left[\frac{\rho_o}{\rho h}\right] \left[\frac{J_n\left(\dfrac{\omega R}{c}\right)}{J_n'\left(\dfrac{\omega R}{c}\right)} \right] \Omega, \qquad \Omega = \frac{\rho R^2 (1 - \mu^2)}{E} \omega^2 \tag{15}$$

$$Z_m = -\left(\frac{1}{\alpha_{mn}}\right)\left[\frac{\rho_o}{\rho h}\right]\left[\frac{I_n(\alpha_{mn} R)}{I_n'(\alpha_{mn} R)}\right]\Omega, \qquad \text{for } \frac{m\pi}{H} \geqslant \frac{\omega}{c} \tag{16a}$$

and

$$Z_m = -\left(\frac{1}{\alpha_{mn}}\right)\left[\frac{\rho_o}{\rho h}\right]\left[\frac{J_n(\alpha_{mn} R)}{J_n'(\alpha_{mn} R)}\right]\Omega, \qquad \text{for } \frac{m\pi}{H} < \frac{\omega}{c}. \tag{16b}$$

2.4. GENERAL FORMULATION

Substitution of the displacements, their derivatives described by the Fourier series in the open range $0 < z < H$ with corresponding boundary values at the ends, and the hydrodynamic force of equation (14) into equation (1), leads to an explicit relation for the Fourier coefficients B_{on}, C_{on} and a set of equations of A_{mn}, B_{mn} and C_{mn} which are coupled together. The solution of these coupled equations

contain the eight unspecified end quantities u_O, u_H, $\tilde{v}_O$, $\tilde{v}_H$, $\tilde{w}_O$, $\tilde{w}_H$, $\tilde{\tilde{w}}_O$ and $\tilde{\tilde{w}}_H$ as follows:

$$B_{on} = \zeta_1(u_O + u_H) + \zeta_2(\tilde{v}_O + \tilde{v}_H) + \zeta_3(\tilde{w}_O + \tilde{w}_H) + \zeta_4(\tilde{\tilde{w}}_O + \tilde{\tilde{w}}_H), \tag{17a}$$

$$C_{on} = \zeta_5(u_O + u_H) + \zeta_6(\tilde{v}_O + \tilde{v}_H) + \zeta_7(\tilde{w}_O + \tilde{w}_H) + \zeta_8(\tilde{\tilde{w}}_O + \tilde{\tilde{w}}_H), \tag{17b}$$

$$\begin{bmatrix} a_1m^2 + a_2 & -a_3m & -a_4m \\ -a_3m & a_5m^2 + a_6 & a_7m^2 + a_8 \\ -a_4m & a_7m^2 + a_8 & -a_9m^4 + a_{10}m^2 + a_{11} - Z_m \end{bmatrix} \begin{bmatrix} A_{mn} \\ B_{mn} \\ C_{mn} \end{bmatrix}$$

$$= \begin{bmatrix} -a_1m[u_O + (-1)^m u_H] \\ a_3[u_O + (-1)^m u_H] + a_5[\tilde{v}_O + (-1)^m \tilde{v}_H] + a_7[\tilde{w}_O + (-1)^m \tilde{w}_H] \\ a_4[u_O + (-1)^m u_H] + a_7[\tilde{v}_O + (-1)^m \tilde{v}_H] + a_{10}[\tilde{w}_O + (-1)^m \tilde{w}_H] \\ + a_9[\tilde{\tilde{w}}_O + (-1)^m \tilde{\tilde{w}}_H - m^2\tilde{w}_O - m^2(-1)^m \tilde{w}_H] \end{bmatrix}. \tag{18}$$

The end forces $N_{z\theta}$ and Q_z of the shell can be written in terms of the unspecified boundary quantities u_O, u_H, $\tilde{v}_O$, $\tilde{v}_H$, $\tilde{w}_O$, $\tilde{w}_H$, $\tilde{\tilde{w}}_O$ and $\tilde{\tilde{w}}_H$ by the substitution of equation (3).

$$N_{z\theta}(0, \theta) = [q_1u_O + q_2\tilde{v}_O + q_3\tilde{w}_O] \sin n\theta, \tag{19a}$$

$$N_{z\theta}(H, \theta) = -[q_1u_H + q_2\tilde{v}_H + q_3\tilde{w}_H] \sin n\theta, \tag{19b}$$

$$Q_z(0, \theta) = [q_4u_O + q_5\tilde{v}_O + q_6\tilde{w}_O + q_7\tilde{\tilde{w}}_O] \cos n\theta, \tag{19c}$$

$$Q_z(H, \theta) = -[q_4u_H + q_5\tilde{v}_H + q_6\tilde{w}_H + q_7\tilde{\tilde{w}}_H] \cos n\theta, \tag{19d}$$

where the coefficient q_i ($i = 1, 2, \ldots, 7$) derived from equation (3) is specified in Appendix B. The boundary values of the displacements and their derivatives, $\tilde{v}_O$, $\tilde{v}_H$, $\tilde{\tilde{w}}_O$ and $\tilde{\tilde{w}}_H$, can be given in combination of the boundary values of u, $\tilde{w}$, $N_{z\theta}$ and Q_z by equation (19), as written by the form:

$$\tilde{v}_O = [g_1u_O + g_2\tilde{w}_O + g_3N^O_{z\theta}], \qquad \tilde{v}_H = [g_1u_H + g_2\tilde{w}_H + g_3N^H_{z\theta}], \tag{20a, b}$$

$$\tilde{\tilde{w}}_O = [g_4u_O + g_5\tilde{w}_O + g_6N^O_{z\theta} + g_7Q^O_z],$$

$$\tilde{\tilde{w}}_H = [g_4u_H + g_5\tilde{w}_H + g_6N^H_{z\theta} + g_7Q^H_z], \tag{20c, d}$$

where the derived coefficients g_i ($i = 1, 2, \ldots, 7$) are also listed in Appendix B. Substitution of equation (20) into equations (17) and (18) gives equations (21) and (22), respectively. Finally, the Fourier coefficients can be defined by u, $\tilde{w}$, $N_{z\theta}$ and Q_z instead of $\tilde{v}$ and $\tilde{\tilde{w}}$.

$$B_{on} = \beta_1(u_O + u_H) + \beta_2(\tilde{w}_O + \tilde{w}_H) + \beta_3(N^O_{z\theta} + N^H_{z\theta}) + \beta_4(Q^O_z + Q^H_z), \tag{21a}$$

$$C_{on} = c_1(u_O + u_H) + c_2(\tilde{w}_O + \tilde{w}_H) + c_3(N^O_{z\theta} + N^H_{z\theta}) + c_4(Q^O_z + Q^H_z). \tag{21b}$$

$$\begin{bmatrix} A_{mn} \\ B_{mn} \\ C_{mn} \end{bmatrix} = \begin{bmatrix} f_{a1} & f_{a2} & f_{a3} & f_{a4} \\ f_{b1} & f_{b2} & f_{b3} & f_{b4} \\ f_{c1} & f_{c2} & f_{c3} & f_{c4} \end{bmatrix} \begin{bmatrix} \{u_O + (-1)^m u_H\} \\ \{\tilde{w}_O + (-1)^m \tilde{w}_H\} \\ \{N^O_{z\theta} + (-1)^m N^H_{z\theta}\} \\ \{Q^O_z + (-1)^m Q^H_z\} \end{bmatrix}. \tag{22}$$

The geometric boundary conditions that must be satisfied are associated with the dynamic displacements v and w. Hence, for arbitrary n it follows that:

$$v(0) = B_{on} + \sum_{m=1}^{\infty} B_{mn} = 0, \qquad v(H) = B_{on} + \sum_{m=1}^{\infty} B_{mn}(-1)^m = 0, \quad (23a, b)$$

$$w(0) = C_{on} + \sum_{m=1}^{\infty} C_{mn} = 0, \qquad w(H) = C_{on} + \sum_{m=1}^{\infty} C_{mn}(-1)^m = 0. \quad (23c, d)$$

The natural boundary conditions that must be zero, are $N_z = 0$ and $M_z = 0$ at both ends of the shell. Substitution of the displacements set and their derivatives into these equations yields the following:

$$\left(\frac{\pi}{H}\right)\left(\frac{u_O + u_H}{2}\right) + \left(\frac{\mu}{R}\right)(n\, B_{on} + C_{on}) + \sum_{m=1}^{\infty}\left[\left(\frac{\pi}{H}\right)\{u_O + (-1)^m u_H + m\, A_{mn}\} + \left(\frac{\mu}{R}\right)\{n\, B_{mn} + C_{mn}\}\right] = 0, \quad (24a)$$

$$\left(\frac{\pi}{H}\right)\left(\frac{u_O + u_H}{2}\right) + \left(\frac{\mu}{R}\right)(n\, B_{on} + C_{on}) + \sum_{m=1}^{\infty}\left[\left(\frac{\pi}{H}\right)\{u_O + (-1)^m u_H + m\, A_{mn}\} + \left(\frac{\mu}{R}\right)\{n\, B_{mn} + C_{mn}\}\right](-1)^m = 0, \quad (24b)$$

$$-\left(\frac{\pi}{H}\right)^2\left(\frac{\tilde{w}_O + \tilde{w}_H}{2}\right) + \left(\frac{\mu}{R^2}\right)n(B_{on} + n\, C_{on}) + \sum_{m=1}^{\infty}\left[-\left(\frac{\pi}{H}\right)^2\{\tilde{w}_O + (-1)^m \tilde{w}_H - m^2\, C_{mn}\} + \left(\frac{\mu}{R^2}\right)n\{B_{mn} + n\, C_{mn}\}\right] = 0, \quad (24c)$$

$$-\left(\frac{\pi}{H}\right)^2\left(\frac{\tilde{w}_O + \tilde{w}_H}{2}\right) + \left(\frac{\mu}{R^2}\right)n(B_{on} + n\, C_{on}) + \sum_{m=1}^{\infty}\left[-\left(\frac{\pi}{H}\right)^2\{\tilde{w}_O + (-1)^m \tilde{w}_H - m^2\, C_{mn}\} + \left(\frac{\mu}{R^2}\right)n\{B_{mn} + n\, C_{mn}\}\right](-1)^m = 0. \quad (24d)$$

The frequency determinant can now be constructed. Substitution of equations (21) and (22) for the coefficients B_{on}, C_{on}, A_{mn}, B_{mn} and C_{mn} into the eight constraint conditions which come from the geometric and natural boundary conditions written as equations (23) and (24), leads to a homogeneous matrix equation:

$$\begin{bmatrix} e_{11} & e_{12} & e_{13} & e_{14} & e_{15} & e_{16} & e_{17} & e_{18} \\ e_{12} & e_{11} & e_{14} & e_{13} & e_{16} & e_{15} & e_{18} & e_{17} \\ e_{21} & e_{22} & e_{23} & e_{24} & e_{25} & e_{26} & e_{27} & e_{28} \\ e_{22} & e_{21} & e_{24} & e_{23} & e_{26} & e_{25} & e_{28} & e_{27} \\ e_{31} & e_{32} & e_{33} & e_{34} & e_{35} & e_{36} & e_{37} & e_{38} \\ e_{32} & e_{31} & e_{34} & e_{33} & e_{36} & e_{35} & e_{38} & e_{37} \\ e_{41} & e_{42} & e_{43} & e_{44} & e_{45} & e_{46} & e_{47} & e_{48} \\ e_{42} & e_{41} & e_{44} & e_{43} & e_{46} & e_{45} & e_{48} & e_{47} \end{bmatrix} \begin{bmatrix} u_O \\ u_H \\ \tilde{w}_O \\ \tilde{w}_H \\ N^O_{z\theta} \\ N^H_{z\theta} \\ Q^O_z \\ Q^H_z \end{bmatrix} = \{0\}. \tag{25}$$

The elements of the matrix, e_{ij} ($i = 1, 2, \ldots, 4$, $j = 1, 2, \ldots, 8$) obtained from equation (24) are listed in Appendix C. Each element of the frequency determinant e_{ij} ($i = 1, 2, \ldots, 4$ and $j = 1, 2, \ldots, 8$) contains an infinite series expansion. For a non-trivial solution of equation (25), the determinant of the matrix, det $[e_{ij}]$ must vanish. This requirement gives a characteristic equation whose eigenvalues correspond to the natural frequencies of the fluid-coupled shell. The corresponding eigenvectors determine the vibrational mode shapes. From the development of these equations there exist two restrictions, as depicted by Chung [13]. The first restriction in this method is $\sigma \neq 0$. When the coefficient σ in Appendix B is zero, the derived coefficients ζ_j ($j = 1, 2, \ldots, 8$) in Appendix B are invalid. However, the other restriction reported by Chung [13], namely $n \neq 0$, is no longer effective in this method, because the coefficients ζ_j in Appendix B maintain a non-zero value for the axisymmetric mode ($n = 0$) shell vibration. Therefore, the natural frequencies of axisymmetric breathing vibrational mode ($n = 0$) can be obtained using this method. The second restriction of this method is $\Delta_{mn} \neq 0$. When the coefficient Δ_{mn} in Appendix B is zero, the derived coefficients a_α, a_β, a_γ, b_β, b_γ and c_γ in Appendix B are invalid. These two restrictions of the analytical method are not serious drawbacks, since most fluid-filled cylindrical shells with general geometric configurations are solvable except for the shells with a particular geometric configuration where $\Delta_{mn} = 0$ or $\sigma = 0$.

2.5. FREQUENCY DETERMINANT

The requirements needed to satisfy the boundary conditions at both ends of the shell lead to an 8×8 frequency determinant. From this determinant, one can also obtain the frequency equation with an order $\leqslant 6$ for any specific combination of boundary conditions among possible cases.

When the shell is clamped at both ends, the associated boundary conditions are given by equation (2). Among these boundary conditions, the two geometric boundary conditions, $v = 0$ and $w = 0$ at $z = 0$ and $z = H$, are not automatically satisfied by equation (5). Therefore the first, second, third and fourth rows of the

matrix in equation (25) are enforced and the terms associated with u_O, u_H, $\tilde{w}_O$, and $\tilde{w}_H$ are released. The 4×4 frequency determinant is obtained from equation (25) by retaining the rows and columns associated with $N^O_{z\theta}$, $N^H_{z\theta}$, Q^O_z and Q^H_z:

$$\begin{vmatrix} e_{15} & e_{16} & e_{17} & e_{18} \\ e_{16} & e_{15} & e_{18} & e_{17} \\ e_{25} & e_{26} & e_{27} & e_{28} \\ e_{26} & e_{25} & e_{28} & e_{27} \end{vmatrix} = 0. \tag{26}$$

As a typical case involving the enforcement of geometric boundary conditions and the release of unwanted natural boundary conditions, consider the simply supported shell with axial constraints at both ends. The associated boundary conditions are:

$$u = 0, \qquad v = 0, \qquad w = 0, \qquad M_z = 0, \qquad \text{at } z = 0 \quad \text{and } z = H. \tag{27}$$

The modal functions set of equation (5) automatically satisfies $u = 0$ at $z = 0$ and $z = H$ but the four geometric boundary conditions $v = 0$ and $w = 0$ at $z = 0$ and $z = H$ are not automatically satisfied by the modal functions set. In addition, the natural boundary conditions $M_z = 0$, at $z = 0$ and $z = H$ in equations (24c) and (24d) must be satisfied. Therefore, the first, second, third, fourth, seventh and eighth rows of the matrix in equation (25) are enforced at the same time, and the terms associated with u_O and u_H are released. The frequency equation can be found from the geometrical constraint of $u = 0$ at both ends, at the same time, with the end displacements and forces $\tilde{w}$, $N_{z\theta}$, Q_z left unspecified. This is effectively done in equation (25) by retaining the rows and columns associated with $\tilde{w}_O$, $N^O_{z\theta}$, Q^O_z, $\tilde{w}_H$, $N^H_{z\theta}$ and Q^H_z. The frequency determinant reduced from equation (25) leads to a 6×6 determinant:

$$\begin{vmatrix} e_{13} & e_{14} & e_{15} & e_{16} & e_{17} & e_{18} \\ e_{14} & e_{13} & e_{16} & e_{15} & e_{18} & e_{17} \\ e_{23} & e_{24} & e_{25} & e_{26} & e_{27} & e_{28} \\ e_{24} & e_{23} & e_{26} & e_{25} & e_{28} & e_{27} \\ e_{43} & e_{44} & e_{45} & e_{46} & e_{47} & e_{48} \\ e_{44} & e_{43} & e_{46} & e_{45} & e_{48} & e_{47} \end{vmatrix} = 0. \tag{28}$$

The case of a simply supported–clamped shell involves the enforcement and release of geometrical and natural boundary conditions. The boundary conditions of the simply supported–clamped shell are given as:

$$u = 0, \qquad v = 0, \qquad w = 0, \qquad \text{at } z = 0, \qquad H \qquad \text{and } M_z = 0, \qquad \text{at } z = 0,$$
$$w_{,z} = 0 \qquad \text{at } z = H. \tag{29}$$

Among these boundary conditions, the geometric boundary conditions $u = 0$ at $z = 0$ and $z = H$ are automatically satisfied by the modal functions set of equation (5), and the four geometric boundary conditions $v = 0$ and $w = 0$ at $z = 0$ and $z = H$ are not automatically satisfied by the modal functions set. In addition, the

natural boundary condition $M_z = 0$ at $z = 0$ in equation (24c) must be satisfied. Therefore, the first, second, third, fourth and seventh rows of the matrix in equation (25) are enforced at the same time, and the terms associated with u_O, u_H and $\tilde{w}_H$ are released. The frequency equation can be found from the geometrical constraints of u_O, u_H and $\tilde{w}_O$, at the same time, with $\tilde{w}_H$ and the end displacements and forces, $N_{z\theta}$ and Q_z, left unspecified. This is effectively done in equation (25) by retaining the rows and columns associated with $N^O_{z\theta}$, Q^O_z, $\tilde{w}_H$, $N^H_{z\theta}$ and Q^H_z. The frequency determinant reduced from equation (25) leads to a 5×5 determinant:

$$\begin{vmatrix} e_{14} & e_{15} & e_{16} & e_{17} & e_{18} \\ e_{13} & e_{16} & e_{15} & e_{18} & e_{17} \\ e_{24} & e_{25} & e_{26} & e_{27} & e_{28} \\ e_{23} & e_{26} & e_{25} & e_{28} & e_{27} \\ e_{44} & e_{45} & e_{46} & e_{47} & e_{48} \end{vmatrix} = 0. \tag{30}$$

3. EXAMPLE

3.1. CONVERGENCE TESTS FOR FINITE ELEMENT MESH SIZE AND SERIES EXPANSIONS

On the basis of the preceding analysis, equation (26) is numerically solved for the clamped–clamped boundary condition in order to find the coupled natural frequencies of a circular cylindrical shell filled with bounded compressible fluid. In order to check the validity and accuracy of the results from the theoretical study and compare them to the FEM results, computation is carried out for the fluid-coupled system. The cylindrical shell is made of aluminum, having a mean radius of 100 mm, a length of 300 mm, and a wall thickness of 2 mm. The physical properties of the material are as follows: Young's modulus = 69·0 GPa, Poisson's ratio = 0·3, and mass density = 2700 kg/m^3. Water is used as the contained fluid, having a density of 1000 kg/m^3. The sound speed in water is 1483 m/s, which is equivalent to the bulk modulus of elasticity of 2·2 GPa. The clamped boundary condition at both ends of the shell is considered among the possible combinations of boundary conditions described in equation (25). The frequency equations derived in the preceding sections involve an infinite series of algebraic terms. Before exploring the analytical method to obtain the coupled natural frequencies of the compressible fluid-filled shell, it is necessary to conduct convergence studies and establish the number of terms which are required in the series expansions involved. In the numerical calculation, the Fourier expansion term m is set at 100, which gives an exact enough solution by convergence. In general, the solution approaches the exact frequency from above as the number of terms included in the series increases. However, the use of more than 100 terms does not improve the solutions significantly.

Finite element analyses using a commercial computer code, ANSYS software (version 5.2) are performed to verify the results of the theoretical study. In order to obtain exact FEM results which can be used as baseline data, convergence

studies are conducted, as shown in Table 1, by gradually increasing the mesh size. In finite elements analyses, two-dimensional axisymmetric models are constructed with axisymmetric two-dimensional fluid elements (FLUID81) and axisymmetric shell elements (SHELL61). The fluid region is divided into a number of identical fluid elements with four nodes. We model the circular cylindrical shell as deformable shell elements with two nodes. The fluid boundary conditions at the top and bottom of the shell have zero displacement and rotation. The nodes which are connected entirely by the fluid elements are free to move arbitrarily in three-dimensional space, with the exception of those restricted to motion in a symmetric center line. That is, the radial displacement of the fluid element nodes at $r = 0$ is constrained, and the bottom and top surfaces of the fluid cavity are considered to be fixed in the axial direction for the bounded fluid model. The radial velocity of the fluid nodes along the wetted shell surface coincides to that of the shell. However, no constraint is applied to the free surface nodes of the fluid elements for the sloshing fluid model. We investigate the fluid bounding effect on the natural frequencies by comparing it with the case of the free fluid surface at the top of the shell. Finally, in the natural frequency calculation, the fluid compressibility is varied in order to study its effect on the coupled natural frequencies of the shell filled with bounding fluid.

Table 1 will make it easier to check the convergence of frequencies and compare the theoretical frequencies with the corresponding FEM ones. As the fluid and shell meshes are increased, most of the natural frequencies converge to the exact values. The coupled natural frequencies obtained from the FEM converge rapidly, except for the higher axial mode numbers. In order to get more accurate results for the higher axial mode numbers, the mesh size of the two-dimensional FEM model should be increased. Unfortunately, there still exists the unrefined higher modes, even though many low mode frequencies converge by increasing the mesh size. In order to save time, the mesh size is stopped at 12 by 40 elements for the inner fluid region. Although case 5 of the 480 fluid elements and 40 shell elements does not provide exact converged values for the high axial modes, the trend of natural frequencies obtained by the FEM in Table 1 gives insight as to where exactly the converged values are located. The convergence test for five cases in Table 1 can be enough to estimate the validity of the theory.

3.2. VALIDITY OF THE THEORY

Case 5 of Table 1 demonstrates the results from the FEM model, which has 480 (12×40) fluid elements and 40 shell elements. The largest discrepancies between the theoretical and the FEM results are 2·21% for $n = 1$ and $m' = 4$ and 2·02% for $n = 1$ and $m' = 3$. The discrepancy in the table is defined by:

$$\text{Discr. (Discrepancy, \%)} = \left[\frac{\text{theoretical frequency} - \text{frequency obtained by FEM (Case 5)}}{\text{frequency obtained by FEM (Case 5)}}\right] \times 100. \quad (31)$$

TABLE 1

Comparison of FEM and theoretical coupled natural frequencies (Hz) *for a cylindrical shell filled with bounded compressible fluid with* $c = 1483$ m/s

Mode		FEM (Hz)											
		Case 1		Case 2		Case 3		Case 4		Case 5			
n	m'	Fluid 8×10^b	Shell 10^b	Fluid 8×15^b	Shell 15^b	Fluid 8×20^b	Shell 20^b	Fluid 12×30^b	Shell 30^b	Fluid 12×40^b	Shell 40^b	Theory (Hz)	Discrepancy[a] (%)
1	1	1017·6		1014·6		1013·5		1011·0		1010·7		1007·5	−0·32
	2	1768·6		1748·9		1740·3		1726·6		1723·9		1699·5	−1·41
	3	2453·0		2387·5		2358·4		2326·9		2318·2		2271·2	−2·02
	4	3183·8		3028·7		2961·1		2903·6		2884·4		2820·6	−2·21
2	1	733·0		730·1		729·1		728·3		728·1		728·6	0·06
	2	1490·4		1472·7		1465·7		1459·5		1457·8		1453·9	−0·26
	3	2249·6		2192·4		2168·3		2148·3		2141·8		2122·6	−0·89
	4	2981·0		2842·9		2784·7		2740·6		2724·6		2685·6	−1·43
3	1	556·5		553·8		553·0		552·7		552·6		553·0	0·07
	2	1182·8		1166·7		1160·7		1157·4		1156·0		1156·2	0·01
	3	1913·9		1861·7		1840·9		1827·8		1822·5		1816·4	−0·33
	4	2670·6		2545·6		2494·9		2461·7		2448·2		2428·5	−0·80
4	1	519·6		517·2		516·3		516·6		516·4		516·8	0·07
	2	1007·6		993·0		987·8		986·1		984·8		985·5	0·07
	3	1651·4		1604·3		1586·3		1577·4		1572·8		1571·1	−0·10
	4	2381·0		2267·7		2223·3		2198·1		2186·4		2176·5	−0·45
5	1	645·7		643·0		642·1		643·2		643·0		644·0	0·15
	2	994·6		980·4		975·2		974·8		973·5		974·5	0·10
	3	1535·2		1491·2		1474·6		1468·5		1464·3		1464·2	−0·01
	4	2206·8		2102·1		2061·9		2042·3		2031·8		2026·4	−0·26
6	1	905·7		902·4		901·2		904·0		903·7		906·3	0·28
	2	1154·7		1139·2		1133·4		1134·6		1133·2		1135·5	0·20
	3	1594·8		1550·3		1533·5		1529·8		1525·5		1526·7	0·07
	4	2195·8		2094·2		2055·2		2039·6		2029·5		2026·9	−0·12

Note: [a] Discrepancy defined in equation (31). [b] Number of elements

Judging from the trend of Table 1, we can guess that the discrepancies can be reduced by using a fine mesh model rather than a coarse mesh model for the high axial modes. As the coarse mesh of case 1 changes to the fine mesh of case 2 or case 3, all of the natural frequencies get close to the theoretical results. Finally, the natural frequencies of the axial higher vibrational modes obtained by the FEM may approach the theoretical results according to the increase in mesh size. As may be seen, the present results agree quite well with the FEM solution.

Analytical mode shapes for a particular natural frequency can always be investigated by substituting the calculated frequency parameter into the frequency matrix and finding the relative values of unspecified end forces and values, and finally, evaluating the Fourier coefficients of the assumed modal displacement functions. Comparison of the mode shapes between the present method and others was not attempted in this paper.

3.3. BOUNDING EFFECTS

A free surface at the top side of the incompressible fluid region was assumed in most of the previous works. In some studies, the free surface boundary condition of the fluid was sophisticated and in the others, the sloshing of the fluid during vibration was neglected. However, when a compressible fluid is contained in a cylindrical shell with rigid top and bottom plates, the free surface may not exist any more. When the previous methods are pursued in the treatment of this problem, some errors can be given in the special range of modes. In order to investigate the bounding effect of compressible fluid, the coupled natural frequencies for both cases of the bounded fluid and sloshing fluid are acquired by the finite element method and plotted in Figures 2 and 3 for the cases of $c = 1483$ m/s ($B = 2{\cdot}2$ GPa) and $c = 447$ m/s ($B = 0{\cdot}2$ GPa), respectively. Figure 2 shows a difference in the coupled natural frequencies between the cases of bounded and unbounded fluid. It can be observed that the natural frequency of the shell with sloshing fluid is larger than that with bounded fluid, by about 8% for $m' = 3$ and $n = 1$. As one can see, the bounding fluid effect on the natural frequencies is significant for the lower circumferential modes. It is significant that the maximum deviation between the two cases happens at the circumferential mode number $n = 1$. During the vibration of the shell, the hydrodynamic mass for the unbounded case with a free surface is smaller than that for the bounded fluid, because the radial movement of fluid for the bounded fluid is greater than that for the fluid with a free surface in the case of low circumferential modes. However, as the circumferential mode number n increases, the radial movement of fluid will be reduced because a number of circumferential waves of the shell disturbs the long distance movement of fluid during vibration. Therefore, the bounding effect of fluid at the low circumferential modes is dominant. Eventually, the hydrodynamic mass induced by unbounding the top surface of the fluid will increase the natural frequencies. Figure 3 illustrates the differences between cases of bounded fluid and unbounded fluid for more compressible fluid, $c = 447$ m/s. Similar results can be observed. For the case of $c = 447$ m/s, the natural frequencies for $n = 1$ and 2 are less than those of $c = 1483$ m/s. The bounding effect deceases according to the increase of the circumferential mode number, regardless of fluid compressibility.

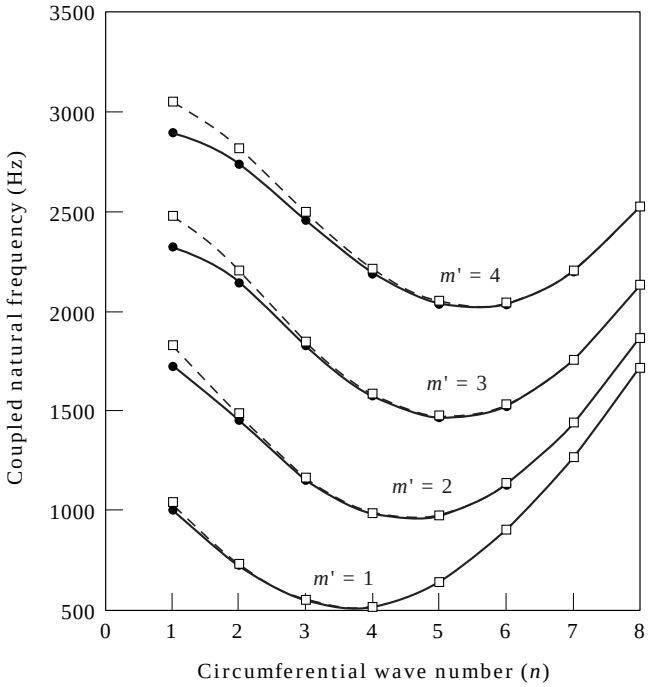

Figure 2. Effects of fluid bounding on the coupled natural frequencies (Hz): sound velocity in a fluid medium for $c = 1483$ m/s (dashed line = the case of fluid with a free surface at the top, continuous line = the case of bounded fluid).

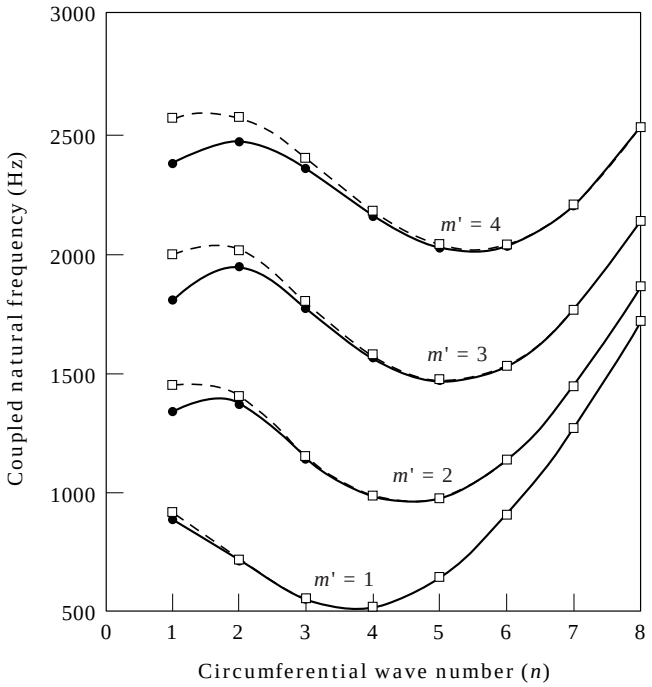

Figure 3. Effects of fluid bounding on the coupled natural frequencies (Hz): sound velocity in a fluid medium for $c = 447$ m/s (dashed line = the case of fluid with a free surface at the top, continuous line = the case of bounded fluid).

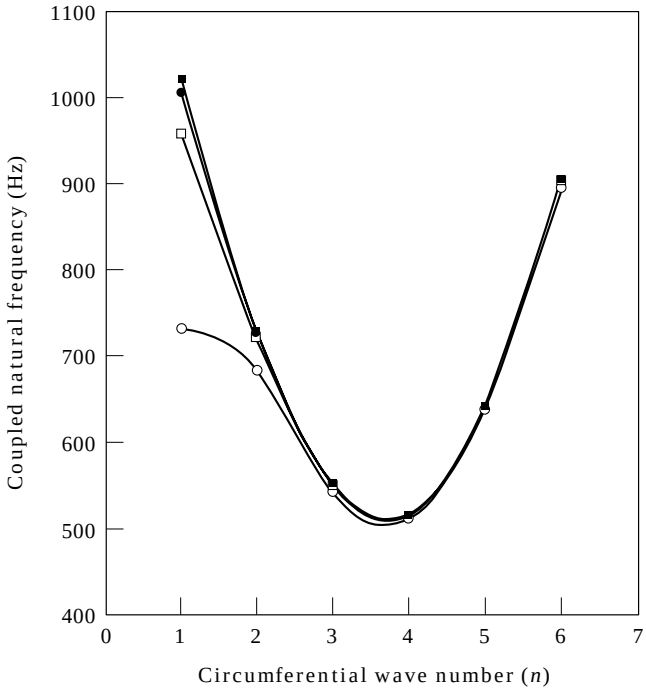

Figure 4. Effects of fluid compressibility on the coupled natural frequencies (Hz) of a cylindrical shell filled with bounded compressible fluid for $m' = 1$. —○—, $c = 331$ m/s; —□—, $c = 800$ m/s; —●—, $c = 1483$ m/s; —■—, $c = 2800$ m/s.

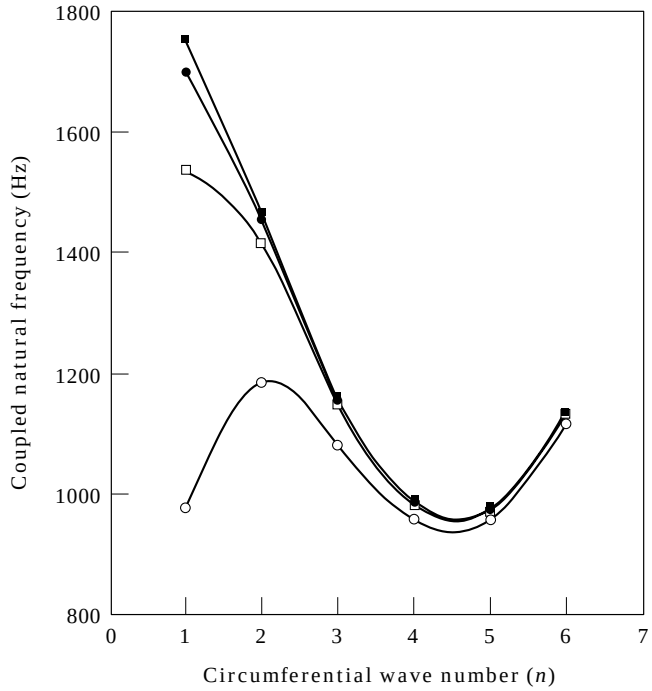

Figure 5. Effects of fluid compressibility on the coupled natural frequencies (Hz) of a cylindrical shell filled with bounded compressible fluid for $m' = 2$. Key as for Figure 4.

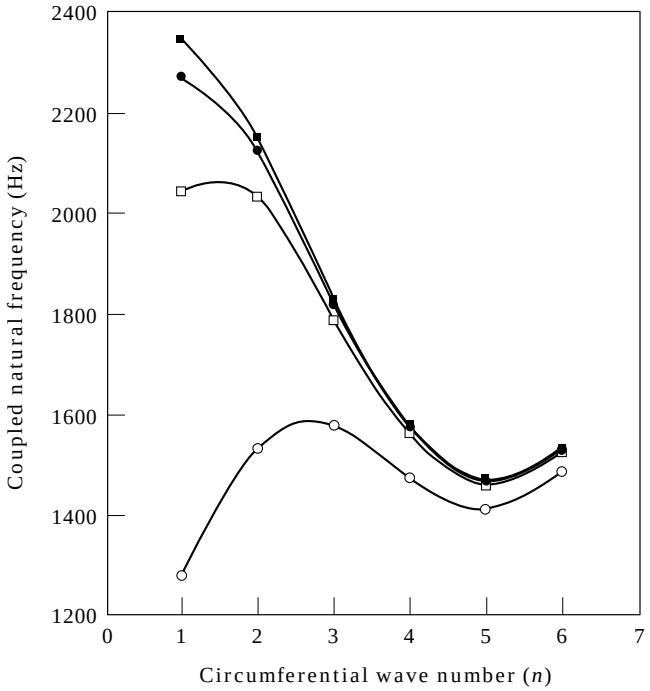

Figure 6. Effects of fluid compressibility on the coupled natural frequencies (Hz) of a cylindrical shell filled with bounded compressible fluid for $m' = 3$. Key as for Figure 4.

The application of a free surface to the bounded fluid case can cause an overestimation of natural frequency at the lower circumferential modes.

3.4. COMPRESSIBILITY EFFECTS

Figures 4–6 illustrate the changes of coupled natural frequencies according to the sound velocity in fluid for the axial mode number $m' = 1$, 2 and 3, respectively. The compressibility effect of the fluid on the natural frequencies is negligible for the high circumferential mode, n, as shown in Figures 4–6. As the compressibility of the fluid increases, the frequencies decrease drastically for the circumferential wave number $n = 1$, regardless of axial mode numbers. It is caused by the combined effects of added mass and stiffness reduction of the compressible fluid. In the case of the incompressible fluid ($c \to \infty$), all the work of the structural displacements on the fluid–shell interface is transformed into kinetic energy of the fluid. The incompressible fluid adds the extra inertial properties to the shell, which is well known as the added mass effect. Similarly, in the case of the compressible fluid, all the work of the shell displacements on the fluid–structure interface is transformed into kinetic and potential energies of the fluid. Decrease of the sound speed in fluid gives a reduction of fluid stiffness due to the diminution of the bulk modulus of elasticity. The effect of reduced fluid stiffness accelerates the effect of its increased mass, especially for the low circumferential mode. It will appear as the decreased coupled frequencies of the system for the low circumferential wave number. However, for the high circumferential wave number, a number of

circumferential waves of fluid counteracts its strokes and added mass. Eventually, the effect of circumferential fluid waves tend to diminish the effect of fluid compressibility on the coupled natural frequencies.

4. CONCLUSIONS

An analytical method to estimate the natural frequencies of a circular cylindrical shell filled with a compressible fluid is developed using the series expansion method based on the finite Fourier transform. To clarify the validity of the analytical method, an example for a clamped–clamped cylindrical shell is examined using the analytical method and the finite element method. Excellent agreement is found between the finite element analysis results and the analytical results, and the analytical method is verified with good accuracy. Moreover, it is found that the effects of compressibility and bounding of fluid on the coupled natural frequencies are significant in the low circumferential vibrational modes. The natural frequencies for a cylindrical shell filled with a bounded fluid are less than those for the cylindrical shell filled with unbounded fluid with a free surface. The decrease of fluid compressibility gives a decrease of natural frequency in the low circumferential wave number n. This analytical method will be useful to the dynamic analysis of a circular cylindrical shell containing a bounded compressible fluid, such as a reactor vessel filled with coolant and a chemical tank filled with compressed gas.

REFERENCES

1. W. E. Stillman 1973 *Journal of Sound Vibration* **30**, 509–524. Free vibration of cylinders containing liquid.
2. N. Yamaki, J. Tani and T. Yamaji 1984 *Journal of Sound Vibration* **94**, 531–550. Free vibration of a clamped–clamped circular cylindrical shell partially filled with liquid.
3. P. B. Gonçalves and N. R. S. S. Ramos 1996 *Journal of Sound and Vibration* **195**, 429–444. Free vibration analysis of cylindrical tanks partially filled with liquid.
4. A. A. Lakis and M. Sinno 1992 *International Journal for Numerical Methods in Engineering* **33**, 235–268. Free vibration of axisymmetric and beam-like cylindrical shells partially filled with liquid.
5. T. Mikami and J. Yoshimura 1992 *Computers and Structures* **44**, 343–351. The collocation method for analyzing free vibration of shells of revolution with either internal or external fluids.
6. R. P. S. Han and J. D. Liu 1994 *Journal of Sound and Vibration* **176**, 235–253. Free vibration analysis of a fluid-loaded variable thickness cylindrical tank.
7. K. H. Jeong and S. C. Lee 1996 *Computers and Structures* **58**, 937–946. Fourier series expansion method for free vibration analysis of either a partially liquid-filled or a partially liquid-surrounded circular cylindrical shell.
8. R. K. Gupta and G. L. Hutchinson 1988 *Journal of Sound and Vibration* **122**, 491–506. Free vibration analysis of liquid storage tanks.
9. F. Zhu 1994 *Journal of Sound and Vibration* **171**, 641–649. Rayleigh quotients for coupled free vibration.
10. Y. Y. Huang 1991 *Journal of Sound and Vibration* **145**, 51–60. Orthogonality of wet modes in coupled vibrations of cylindrical shells containing liquids.

11. S. S. Chen and G. S. Rosenberg 1975 *Nuclear Engineering and Design* **32**, 302–310. Dynamics of a coupled shell–fluid system.
12. T. Mazuch, J. Horacek, J. Trnka and J. Vesely 1996 *Journal of Sound and Vibration* **193**, 669–690. Natural modes and frequencies of a thin clamped–free steel cylindrical storage tank partially filled with water: FEM and measurement.
13. H. Chung 1981 *Journal of Sound and Vibration* **74**, 331–350. Free vibration of circular cylindrical shells.
14. I. N. Sneddon 1951 *Fourier Transforms*. New York: McGraw-Hill Book Company, Inc.

APPENDIX A: MODAL DISPLACEMENT FUNCTIONS AND THEIR DERIVATIVES

$$u(z,\theta)=\left[\sum_{m=1}^{\infty}A_{mn}\sin\left(\frac{m\pi z}{H}\right)\right]\cos n\theta,\qquad 0<z<H,$$

$$u(0,\theta)=-\left(\frac{\pi}{2}\right)u_O\cos n\theta,\qquad u(H,\theta)=\left(\frac{\pi}{2}\right)u_H\cos n\theta,$$

$$u_{,z}(z,\theta)=\left(\frac{\pi}{H}\right)\left[\frac{u_O+u_H}{2}+\sum_{m=1}^{\infty}\{u_O+u_H(-1)^m+m\,A_{mn}\}\cos\left(\frac{m\pi z}{H}\right)\right]\cos n\theta,$$

$$0\leqslant z\leqslant H,$$

$$u_{,zz}(z,\theta)=-\left(\frac{\pi}{H}\right)^2\left[\sum_{m=1}^{\infty}\{u_Om+u_Hm(-1)^m+m^2\,A_{mn}\}\sin\left(\frac{m\pi z}{H}\right)\right]\cos n\theta,$$

$$0<z<H,$$

$$u_{,zz}(0,\theta)=-\left(\frac{\pi^3}{2H^2}\right)\tilde{\tilde{u}}_O\cos n\theta,\qquad u_{,zz}(H,\theta)=\left(\frac{\pi^3}{2H^2}\right)\tilde{\tilde{u}}_H\cos n\theta;$$

$$v(z,\theta)=\left[B_{on}+\sum_{m=1}^{\infty}B_{mn}\cos\left(\frac{m\pi z}{H}\right)\right]\sin n\theta,\qquad 0\leqslant z\leqslant H,$$

$$v_{,z}(z,\theta)=-\left(\frac{\pi}{H}\right)\left[\sum_{m=1}^{\infty}B_{mn}\,m\sin\left(\frac{m\pi z}{H}\right)\right]\sin n\theta,\qquad 0<z<H,$$

$$v_{,z}(0,\theta)=-\left(\frac{\pi^2}{2H}\right)\tilde{v}_O\sin n\theta,\qquad v_{,z}(H,\theta)=\left(\frac{\pi^2}{2H}\right)\tilde{v}_H\sin n\theta,$$

$$v_{,zz}(z,\theta)=\left(\frac{\pi}{H}\right)^2\left[\frac{\tilde{v}_O+\tilde{v}_H}{2}+\sum_{m=1}^{\infty}\{\tilde{v}_O+\tilde{v}_H(-1)^m-m^2B_{mn}\}\cos\left(\frac{m\pi z}{H}\right)\right]\sin n\theta,$$

$$0 \leqslant z \leqslant H,$$

$$w(z, \theta) = \left[C_{on} + \sum_{m=1}^{\infty} C_{mn} \cos\left(\frac{m\pi z}{H}\right)\right] \cos n\theta, \qquad 0 \leqslant z \leqslant H,$$

$$w_{,z}(z, \theta) = -\left(\frac{\pi}{H}\right)\left[\sum_{m=1}^{\infty} C_{mn}\, m \sin\left(\frac{m\pi z}{H}\right)\right] \cos n\theta, \qquad 0 < z < H,$$

$$w_{,z}(0, \theta) = -\left(\frac{\pi^2}{2H}\right)\tilde{w}_O \cos n\theta, \qquad w_{,z}(H, \theta) = \left(\frac{\pi^2}{2H}\right)\tilde{w}_H \cos n\theta,$$

$$w_{,zz}(z, \theta) = \left(\frac{\pi}{H}\right)^2\left[\frac{\tilde{w}_O + \tilde{w}_H}{2} + \sum_{m=1}^{\infty} \{\tilde{w}_O + \tilde{w}_H(-1)^m$$

$$-m^2\, C_{mn}\} \cos\left(\frac{m\pi z}{H}\right)\right] \cos n\theta, \qquad 0 \leqslant z \leqslant H,$$

$$w_{,zzz}(z, \theta) = -\left(\frac{\pi}{H}\right)^3\left[\sum_{m=1}^{\infty} \{\tilde{w}_O m + \tilde{w}_H m(-1)^m - m^3\, C_{mn}\} \sin\left(\frac{m\pi z}{H}\right)\right] \cos n\theta,$$

$$0 < z < H,$$

$$w_{,zzz}(0, \theta) = -\left(\frac{\pi^4}{2H^3}\right)\tilde{\tilde{w}}_O \cos n\theta, \qquad w_{,zzz}(H, \theta) = \left(\frac{\pi^4}{2H^3}\right)\tilde{\tilde{w}}_H \cos n\theta,$$

$$w_{,zzzz}(z, \theta) = \left(\frac{\pi}{H}\right)^4 \left[\left(\frac{\tilde{\tilde{w}}_O + \tilde{\tilde{w}}_H}{2}\right) + \sum_{m=1}^{\infty} \{\tilde{\tilde{w}}_O + (-1)^m \tilde{\tilde{w}}_H - w_O m^2 - w_H m^2(-1)^m$$

$$+m^4 C_{mn}\} \cos\left(\frac{m\pi z}{H}\right)\right] \cos n\theta, \qquad 0 \leqslant z \leqslant H.$$

APPENDIX B: SYMBOLS USED IN EQUATIONS (15)–(22) AND APPENDIX C

$$a_1 = \left(\frac{\pi R}{H}\right)^2, \qquad a_2 = \tfrac{1}{2}(1-\mu)\left(1 + \frac{k}{4}\right)n^2 - \Omega,$$

$$a_3 = -\left(\frac{\pi R}{H}\right)\left[\frac{1+\mu}{2} - \frac{3(1-\mu)}{8}\, k\right] n,$$

$$a_4 = -\left(\frac{\pi R}{H}\right)\left[\mu - \frac{(1-\mu)}{2}kn^2\right], \qquad a_5 = a_1\left[\frac{1-\mu}{2}\right][1 + \tfrac{9}{4}k],$$

$$a_6 = (1+k)n^2 - \Omega, \qquad a_7 = \tfrac{1}{2}a_1(3-\mu)kn, \qquad a_8 = (1+kn^2)n,$$

$$a_9 = -a_1^2 k, \qquad a_{10} = 2a_1 kn^2,$$

$$a_{11} = 1 + kn^4 - \Omega; \qquad Y_1 = -\left(\frac{c}{\omega}\right)\left[\frac{\rho_o}{\rho h}\right]\left[\frac{J_n\left(\frac{\omega R}{c}\right)}{J_n'\left(\frac{\omega R}{c}\right)}\right]\Omega,$$

$$Z_m = -\left(\frac{1}{\alpha_{mn}}\right)\left[\frac{\rho_o}{\rho h}\right]\left[\frac{I_n(\alpha_{mn}R)}{I_n'(\alpha_{mn}R)}\right]\Omega,$$

$$\Omega = \frac{\rho R^2(1-\mu^2)\omega^2}{E}, \qquad \zeta_1 = \frac{(a_{11}-Y_1)a_3 - a_4a_8}{\sigma}, \qquad \zeta_2 = \frac{(a_{11}-Y_1)a_5 - a_7a_8}{\sigma},$$

$$\zeta_3 = \frac{(a_{11}-Y_1)a_7 - a_{10}a_8}{\sigma}, \qquad \zeta_4 = \frac{-a_8a_9}{\sigma}, \qquad \zeta_5 = \frac{a_6a_4 - a_3a_8}{\sigma},$$

$$\zeta_6 = \frac{a_6a_7 - a_5a_8}{\sigma}, \qquad \zeta_7 = \frac{a_6a_{10} - a_7a_8}{\sigma}, \qquad \zeta_8 = \frac{a_6a_9}{\sigma},$$

$$\sigma = 2\{a_6(a_{11} - Y_1) - a_8^2\}, \qquad \sigma \neq 0;$$

$$q_1 = \frac{\pi hEn}{4(1+\mu)R}[1 - \tfrac{3}{4}k], \qquad q_2 = \frac{-\pi^2 hE}{4(1+\mu)H}[1 + \tfrac{9}{4}k], \qquad q_3 = -\frac{3\pi^2 hEkn}{4(1+\mu)H},$$

$$q_4 = \frac{-\pi h^3 En^2}{48(1+\mu)R^3}, \qquad q_5 = \frac{(\mu-3)\pi^2 h^3 En}{48(1-\mu^2)HR^2}, \qquad q_6 = \frac{(\mu-2)\pi^2 h^3 En^2}{24(1-\mu^2)HR^2},$$

$$q_7 = \frac{\pi^4 h^3 E}{24(1-\mu^2)H^3}; \qquad g_1 = \left(\frac{H}{\pi R}\right)\left(\frac{4-3k}{4+9k}\right)n, \qquad g_2 = \frac{12kn}{4+9k},$$

$$g_3 = \frac{-16(1+\mu)}{\pi^2(4+9k)hE}, \qquad g_4 = \left(\frac{H}{\pi R}\right)^3\left[\frac{8-4\mu-3k\mu}{4+9k}\right]n^2,$$

$$g_5 = \left(\frac{H}{\pi R}\right)^2\left[\frac{8-4\mu-27k\mu+72k}{4+9k}\right]n^2, \qquad g_6 = \frac{-8H^3n}{\pi^4 hER^2}\left[\frac{(1+\mu)(3-\mu)}{4+9k}\right],$$

$$g_7 = \frac{24(1-\mu^2)H^3}{\pi^4 h^3 E};$$

$$s_{11} = a_1m^2 + a_2, \qquad s_{12} = -a_3m, \qquad s_{13} = -a_4m, \qquad s_{22} = a_5m^2 + a_6,$$

$$s_{23} = a_7m^2 + a_8, \qquad s_{33} = -a_9m^4 + a_{10}m^2 + a_{11} - Z_m,$$

$$a_\alpha = \frac{s_{22}s_{33} - s_{23}^2}{\Delta_{mn}}, \qquad a_\beta = \frac{s_{13}s_{23} - s_{12}s_{33}}{\Delta_{mn}}, \qquad a_\gamma = \frac{s_{12}s_{23} - s_{13}s_{22}}{\Delta_{mn}},$$

$$b_\beta = \frac{s_{11}s_{33} - s_{13}^2}{\Delta_{mn}}, \qquad b_\gamma = \frac{s_{12}s_{13} - s_{11}s_{23}}{\Delta_{mn}}, \qquad c_\gamma = \frac{s_{11}s_{22} - s_{12}^2}{\Delta_{mn}},$$

$$\Delta_{mn} = \begin{vmatrix} s_{11} & s_{12} & s_{13} \\ s_{12} & s_{22} & s_{23} \\ s_{13} & s_{23} & s_{33} \end{vmatrix}, \qquad \Delta_{mn} \neq 0;$$

$$\beta_1 = \zeta_1 + \zeta_2 g_1 + \zeta_4 g_4, \qquad \beta_2 = \zeta_2 g_2 + \zeta_3 + \zeta_4 g_5, \qquad \beta_3 = \zeta_2 g_3 + \zeta_4 g_6,$$

$$\beta_4 = \zeta_4 g_7, \qquad c_1 = \zeta_5 + \zeta_6 g_1 + \zeta_8 g_4,$$

$$c_2 = \zeta_6 g_2 + \zeta_7 + \zeta_8 g_5, \qquad c_3 = \zeta_6 g_3 + \zeta_8 g_6,$$

$$c_4 = \zeta_8 g_7, \qquad f_{a1} = -a_\alpha m a_1 + a_\beta(a_3 + a_5 g_1) + a_\gamma(a_4 + a_7 g_1 + a_9 g_4),$$

$$f_{b1} = -a_\beta m a_1 + b_\beta(a_3 + a_5 g_1) + b_\gamma(a_4 + a_7 g_1 + a_9 g_4),$$

$$f_{c1} = -a_\gamma m a_1 + b_\gamma(a_3 + a_5 g_1) + c_\gamma(a_4 + a_7 g_1 + a_9 g_4),$$

$$f_{a2} = a_\beta(a_5 g_2 + a_7) + a_\gamma(a_7 g_2 + a_{10} + a_9 g_5 - a_9 m^2),$$

$$f_{b2} = b_\beta(a_5 g_2 + a_7) + b_\gamma(a_7 g_2 + a_{10} + a_9 g_5 - a_9 m^2),$$

$$f_{c2} = b_\gamma(a_5 g_2 + a_7) + c_\gamma(a_7 g_2 + a_{10} + a_9 g_5 - a_9 m^2),$$

$$f_{a3} = a_\beta(a_5 g_3) + a_\gamma(a_7 g_3 + a_9 g_6), \qquad f_{b3} = b_\beta(a_5 g_3) + b_\gamma(a_7 g_3 + a_9 g_6),$$

$$f_{c3} = b_\gamma(a_5 g_3) + c_\gamma(a_7 g_3 + a_9 g_6), \qquad f_{a4} = a_\gamma(a_9 g_7), \qquad f_{b4} = b_\gamma(a_9 g_7),$$

$$f_{c4} = c_\gamma(a_9 g_7).$$

APPENDIX C: ELEMENTS OF FREQUENCY DETERMINANT

$$e_{11} = \beta_1 + \sum_{m=1}^{\infty} f_{b1}, \qquad e_{12} = \beta_1 + \sum_{m=1}^{\infty} f_{b1}(-1)^m, \qquad e_{13} = \beta_2 + \sum_{m=1}^{\infty} f_{b2},$$

$$e_{14} = \beta_2 + \sum_{m=1}^{\infty} f_{b2}(-1)^m,$$

$$e_{15} = \beta_3 + \sum_{m=1}^{\infty} f_{b3}, \qquad e_{16} = \beta_3 + \sum_{m=1}^{\infty} f_{b3}(-1)^m, \qquad e_{17} = \beta_4 + \sum_{m=1}^{\infty} f_{b4},$$

$$e_{18} = \beta_4 + \sum_{m=1}^{\infty} f_{b4}(-1)^m;$$

$$e_{21} = c_1 + \sum_{m=1}^{\infty} f_{c1}, \qquad e_{22} = c_1 + \sum_{m=1}^{\infty} f_{c1}(-1)^m, \qquad e_{23} = c_2 + \sum_{m=1}^{\infty} f_{c2},$$

$$e_{24} = c_2 + \sum_{m=1}^{\infty} f_{c2}(-1)^m,$$

$$e_{25} = c_3 + \sum_{m=1}^{\infty} f_{c3}, \qquad e_{26} = c_3 + \sum_{m=1}^{\infty} f_{c3}(-1)^m, \qquad e_{27} = c_4 + \sum_{m=1}^{\infty} f_{c4},$$

$$e_{28} = c_4 + \sum_{m=1}^{\infty} f_{c4}(-1)^m;$$

$$e_{31} = \frac{\pi}{2H} + \frac{\mu}{R}(\beta_1 n + c_1) + \sum_{m=1}^{\infty}\left[\frac{\pi}{H}\{1 + mf_{a1}\} + \frac{\mu}{R}\{f_{b1}n + f_{c1}\}\right],$$

$$e_{32} = \frac{\pi}{2H} + \frac{\mu}{R}(\beta_1 n + c_1) + \sum_{m=1}^{\infty}\left[\frac{\pi}{H}\{1 + mf_{a1}\} + \frac{\mu}{R}\{f_{b1}n + f_{c1}\}\right](-1)^m,$$

$$e_{33} = \frac{\mu}{R}(\beta_2 n + c_2) + \sum_{m=1}^{\infty}\left[\left(\frac{m\pi}{H}\right)f_{a2} + \frac{\mu}{R}\{f_{b2}n + f_{c2}\}\right],$$

$$e_{34} = \frac{\mu}{R}(\beta_2 n + c_2) + \sum_{m=1}^{\infty}\left[\left(\frac{m\pi}{H}\right)f_{a2} + \frac{\mu}{R}\{f_{b2}n + f_{c2}\}\right](-1)^m,$$

$$e_{35} = \frac{\mu}{R}(\beta_3 n + c_3) + \sum_{m=1}^{\infty}\left[\left(\frac{m\pi}{H}\right)f_{a3} + \frac{\mu}{R}\{f_{b3}n + f_{c3}\}\right],$$

$$e_{36} = \frac{\mu}{R}(\beta_3 n + c_3) + \sum_{m=1}^{\infty}\left[\left(\frac{m\pi}{H}\right)f_{a3} + \frac{\mu}{R}\{f_{b3}n + f_{c3}\}\right](-1)^m,$$

$$e_{37} = \frac{\mu}{R}(\beta_4 n + c_4) + \sum_{m=1}^{\infty}\left[\left(\frac{m\pi}{H}\right)f_{a4} + \frac{\mu}{R}\{f_{b4}n + f_{c4}\}\right],$$

$$e_{38} = \frac{\mu}{R}(\beta_4 n + c_4) + \sum_{m=1}^{\infty}\left[\left(\frac{m\pi}{H}\right)f_{a4} + \frac{\mu}{R}\{f_{b4}n + f_{c4}\}\right](-1)^m;$$

$$e_{41} = \frac{\mu}{R^2}n(\beta_1 + c_1 n) + \sum_{m=1}^{\infty}\left[\frac{\mu}{R^2}nf_{b1} + \left\{\frac{\mu}{R^2}n^2 + \left(\frac{m\pi}{H}\right)^2\right\}f_{c1}\right],$$

$$e_{42} = \frac{\mu}{R^2} n(\beta_1 + c_1 n) + \sum_{m=1}^{\infty} \left[\frac{\mu}{R^2} n f_{b1} + \left\{ \frac{\mu}{R^2} n^2 + \left(\frac{m\pi}{H} \right)^2 \right\} f_{c1} \right] (-1)^m,$$

$$e_{43} = -\frac{1}{2} \left(\frac{\pi}{H} \right)^2 + \frac{\mu n}{R^2} (\beta_2 + c_2 n) + \sum_{m=1}^{\infty} \left[-\left(\frac{\pi}{H} \right)^2 + \frac{\mu}{R^2} n f_{b2} + \left\{ \frac{\mu}{R^2} n^2 + \left(\frac{m\pi}{H} \right)^2 \right\} f_{c2} \right],$$

$$e_{44} = -\frac{1}{2} \left(\frac{\pi}{H} \right)^2 + \frac{\mu n}{R^2} (\beta_2 + c_2 n) + \sum_{m=1}^{\infty} \left[-\left(\frac{\pi}{H} \right)^2 + \frac{\mu}{R^2} n f_{b2} + \left\{ \frac{\mu}{R^2} n^2 + \left(\frac{m\pi}{H} \right)^2 \right\} f_{c2} \right] (-1)^m,$$

$$e_{45} = \frac{\mu n}{R^2} (\beta_3 + c_3 n) + \sum_{m=1}^{\infty} \left[\frac{\mu}{R^2} n f_{b3} + \left\{ \frac{\mu}{R^2} n^2 + \left(\frac{m\pi}{H} \right)^2 \right\} f_{c3} \right],$$

$$e_{46} = \frac{\mu n}{R^2} (\beta_3 + c_3 n) + \sum_{m=1}^{\infty} \left[\frac{\mu}{R^2} n f_{b3} + \left\{ \frac{\mu}{R^2} n^2 + \left(\frac{m\pi}{H} \right)^2 \right\} f_{c3} \right] (-1)^m,$$

$$e_{47} = \frac{\mu n}{R^2} (\beta_4 + c_4 n) + \sum_{m=1}^{\infty} \left[\frac{\mu}{R^2} n f_{b4} + \left\{ \frac{\mu}{R^2} n^2 + \left(\frac{m\pi}{H} \right)^2 \right\} f_{c4} \right],$$

$$e_{48} = \frac{\mu n}{R^2} (\beta_4 + c_4 n) + \sum_{m=1}^{\infty} \left[\frac{\mu}{R^2} n f_{b4} + \left\{ \frac{\mu}{R^2} n^2 + \left(\frac{m\pi}{H} \right)^2 \right\} f_{c4} \right] (-1)^m.$$

APPENDIX D: NOMENCLATURE

$A_{mn}, B_{on}, C_{on}, B_{mn}, C_{mn}$	Fourier coefficients associated with modal displacement functions of shell
$a_1, a_2, \ldots, a_{11}$	derivable quantities defined in equation (18)
c	sound speed in fluid medium
$c_1, c_2 \ldots, c_4$	derivable quantities defined in equation (21b)
D	extensional rigidity, $Eh/(1-\mu^2)$
D_{on}, D_{mn}	Fourier coefficients associated with fluid motion
$e_{11}, e_{12}, \ldots, e_{48}$	elements of frequency determinant defined in equations (26) and (28)
$g_1, g_2, \ldots, g_7$	derivable quantities defined in equation (20)
K	flexural rigidity, $Eh^3/12(1-\mu^2)$
k	$h^2/12R^2$

M_z	bending moment per unit length
m	Fourier components in axial direction
m'	axial mode number
$N_{z\theta}$	effective membrane shear force per unit length
N_z	membrane tensile force per unit length
n	circumferential mode number
p	hydrodynamic pressure along the inner wall surface of shell
Q_z	effective transverse shear force per unit length
$q_1, q_2, \ldots, q_7$	derivable quantities defined in equation (19)
R, H, h, ρ, μ	mean radius, height thickness, density and Poisson's ratio of shell
t	time
u, v, w	axial, tangential, and radial dynamic displacements and modal functions of shell
Y_1	quantity associated with hydrodynamic pressure on the shell surface defined in equation (15)
Z_m	quantity associated with hydrodynamic pressure on the shell surface defined in equation (16)
z, θ, r	axial, tangential, and radial co-ordinates
$\beta_1, \beta_2, \ldots, \beta_4$	derivable quantities defined in equation (21a)
γ^2	$\rho R^2(1-\mu^2)/E$
Φ, ϕ	general and spatial velocity potentials of fluid defined in equations (6) and (7)
f_{aj}, f_{bj}, f_{cj}	derivable quantities defined in equation (22), where $j = 1 \sim 4$
ρ_o	fluid density
$\zeta_1, \zeta_2, \ldots, \zeta_8$	derivable quantities defined in equation (21)
ω	natural frequency of shell

Subscript or superscript O denotes the value at $z = 0$.
Subscript or superscript H denotes the value at $z = H$.